Herrmann, T. R., Jayaweera, A. R., & Shamoo, A. E. (1986) *Biochemistry 25*, 5834–5838.
Horrocks, W. DeW., Jr., & Sudnick, D. R. (1981) *Acc. Chem. Res. 14*, 384–392.
Horrocks, W. DeW., Jr., & Albin, M. (1984) *Prog. Inorg. Chem. 31*, 1–103.
Hufner, S. (1978) *Optical Spectra of Transparent Rare Earth Compounds*, Academic, New York.
Jorgensen, C. K. (1979) *Handbook on the Physics and Chemistry of Rare Earths* (Gschneidner, K. A., Jr., & Eyring, L., Eds.) Vol. 3, Chapter 23, North-Holland, Amsterdam.
Leventis, R., Gagné, J., Fuller, N., Rand, R. P., & Silvius, J. R. (1986) *Biochemistry 25*, 6978–6987.
Liao, M.-J., & Prestegard, J. H. (1980) *Biochim. Biophys. Acta 601*, 453–461.
MacDonald, P. M., & Seelig, J. (1987) *Biochemistry 26*, 6292–6298.
McIntosh, T. J. (1980) *Biophys. J. 29*, 237–246.
McLaughlin, A. (1982) *Biochemistry 21*, 4879–4885.
Miner, V. W., & Prestegard, J. (1984) *Biochim. Biophys. Acta 774*, 227–236.
Reid, M. F., & Richardson, F. S. (1984) *J. Phys. Chem. 88*, 3579–3586.
Saris, N.-E. L. (1983) *Chem. Phys. Lipids 34*, 1–5.
Smaal, E. B., Mandersloot, J. G., Demal, R. A., de Kruijff, B., & de Gier, J. (1987a) *Biochim. Biophys. Acta 897*, 180–190.
Smaal, E. B., Schreuder, C., van Baal, J. B., Tijberg, P. N. M., Mandersloot, J. G., de Kruijff, B., & de Gier, J. (1987b) *Biochim. Biophys. Acta 897*, 191–196.
Sundler, R., & Papahadjopoulos, D. (1981) *Biochim. Biophys. Acta 649*, 743–750.
Sundler, R., Duzgunes, N., & Papahadjopoulos, D. (1981) *Biochim. Biophys. Acta 649*, 751–758.
Verkleij, A. J. (1984) *Biochim. Biophys. Acta 779*, 43–63.
Wilschut, J., Schloma, J., Bental, M., Hoekstra, D., & Nir, S. (1985) *Biochim. Biophys. Acta 821*, 45–55.

Magnetization of the Sulfite and Nitrite Complexes of Oxidized Sulfite and Nitrite Reductases: EPR Silent Spin $S = {}^1/_2$ States†

Edmund P. Day,*,‡ Jim Peterson,‡ Jacques J. Bonvoisin,‡ Lawrence J. Young,§ James O. Wilkerson,§ and Lewis M. Siegel§

Gray Freshwater Biological Institute, University of Minnesota, P.O. Box 100, Navarre, Minnesota 55392, and Department of Biochemistry, Duke University Medical Center and Veterans Administration Hospital, Durham, North Carolina 27705

Received August 20, 1987

ABSTRACT: The saturation magnetizations of the sulfite complex of oxidized sulfite reductase and the nitrite complex of oxidized nitrite reductase have been measured to determine their spin state. Each shows the saturation magnetization signal of a spin $S = {}^1/_2$ state with $\sum g^2 = 16$, which is typical of low-spin ferrihemes. However, the EPR spectra of these complexes lack the expected signal intensity of a spin $S = {}^1/_2$ state. Indeed, one of these complexes is EPR silent. The reasons for this unexpectedly low EPR signal intensity are considered.

Sulfite reductase (SiR)[1] and nitrite reductase (NiR) are water-soluble enzymes. Each is capable of catalyzing either the six-electron reductions of sulfite to sulfide and nitrite to ammonia or the two-electron reduction of hydroxylamine to ammonia. The holoprotein of NADPH-sulfite reductase of *Escherichia coli* (EC 1.8.1.2; hydrogen sulfide:NADP$^+$ oxidoreductase) is a large (M_r 685 000) oligomeric hemoflavoprotein ($\alpha_8\beta_4$) (Siegel & Davis, 1974). The β subunit (M_r 54 600), denoted the sulfite reductase heme protein (SiR-HP), is catalytically active when reduced methylviologen (MV^+) is used as the reductant (Siegel et al., 1982). Spinach NiR (EC 1.7.7.1; ammonia:ferredoxin oxidoreductase) is very similar to SiR-HP, both in size (M_r 61 000) and in the composition of its active site (Lancaster et al., 1979).

The active site of SiR-HP consists of a siroheme (Murphy et al., 1974) antiferromagnetically exchange coupled (Christner et al., 1981) to a [4Fe-4S] cluster (Siegel, 1978). Antiferromagnetic exchange coupling is good evidence for a bridging ligand, provided the coupling is sufficiently strong ($-2J > 10$ cm^{-1}). ENDOR spectroscopy (Cline et al., 1985) argues against a nitrogenous base, such as a histidine imidazole group, as the bridging ligand between the heme and the [4Fe-4S] cluster. X-ray crystallographic studies (McRee et al., 1986) indicate that the bridge could be either a sulfur or an oxygen atom of an unidentified amino acid side chain.

Mössbauer studies of ^{57}Fe-enriched SiR-HP have established that the exchange coupling between the siroheme and the [4Fe-4S] cluster is maintained in each of three redox states and upon ligation with CN$^-$, CO, NO, or S^{2-} (Christner et al., 1983a,b, 1984). These results, and the observations that the siroheme is five-coordinate (Cline et al., 1985) and near the surface of SiR-HP with the unoccupied sixth position exposed to solvent (McRee et al., 1986), lead to the idea that exogenous

†Supported by National Institutes of Health Grants GM32394 (E.P.D.) and GM32210 (L.M.S.) and Veterans Administration Project Grant 7875-01 (L.M.S.).

‡Gray Freshwater Biological Institute.
§Duke University Medical Center and Veterans Administration Hospital.

[1] Abbreviations: EDTA, ethylenediaminetetraacetic acid; EPR, electron paramagnetic resonance; MV^+, singly reduced methylviologen dication; NADPH, nicotinamide adenine dinucleotide phosphate; NiR, spinach nitrite reductase; SiR, NADPH-sulfite reductase from *E. coli*; SiR-HP, the heme protein subunit of NADPH-sulfite reductase from *E. coli*; SQUID, superconducting quantum interference device; ENDOR, electron nuclear double resonance; DEAE, diethylaminoethyl.

0006-2960/88/0427-2126$01.50/0

ligands bind to the vacant sixth coordination position of the siroheme without disrupting the bridge.

Detailed information is not available for NiR primarily because it is difficult to enrich spinach in ^{57}Fe for Mössbauer study. However, we may infer that the ligand-binding properties of the SiR-HP and NiR are analogous, due to the similarity of the EPR and optical spectra of their ligand adducts (Wilkerson et al., 1983).

The complexes of SiR-HP and NiR with their physiological substrates sulfite and nitrite are of particular interest in understanding the catalytic mechanism(s) of the native enzymes. The sulfite complex of oxidized SiR-HP (and the sulfite complex of NiR that will not be covered here) is also interesting because it is rare that sulfite binds to an oxidized heme protein (Young & Siegel, 1988).

Formation of the sulfite complex of oxidized SiR-HP ($SiR\text{-}HP^0\cdot SO_3^{2-}$)[2] by addition of sulfite to the oxidized enzyme causes the optical absorption spectrum to undergo changes indicative of a transition from high-spin ferric ($S = {}^5/_2$) to low-spin ferric ($S = {}^1/_2$) siroheme (Janick et al., 1983). Surprisingly, the EPR spectrum of the sulfite adduct shows little evidence of the spin $S = {}^1/_2$ state (Siegel et al., 1982; Young & Siegel, 1988). The shift in the optical spectrum of NiR upon formation of the nitrite complex of oxidized NiR ($NiR^0\cdot NO_2^-$) is similar to the shift in the optical spectrum of SiR-HP induced by the formation of $SiR\text{-}HP^0\cdot SO_3^{2-}$. This species ($NiR^0\cdot NO_2^-$), too, is EPR silent (Vega & Kamin, 1977).

We have studied the saturation magnetizations of the sulfite and nitrite complexes of SiR-HP and NiR to determine the spin state of these adducts. In each case the spin is $S = {}^1/_2$, and the form of the saturation magnetization curve indicates that $\sum g^2 = 16$ with $3.5 > g_z > 2.7$. This is typical of low-spin ferriheme complexes (Salerno & Leigh, 1984). However, the typical low-spin ferriheme has an EPR signal intensity corresponding to one spin per molecule.

The nitrite complex of $SiR\text{-}HP^0$ and the sulfite complex of NiR^0 (not specifically considered here) are also EPR silent. The lack of an EPR signal for each of these spin $S = {}^1/_2$ states of the sulfite and nitrite complexes of these siroheme metalloproteins is difficult to understand. Several possible explanations for the missing EPR signal intensity will be examined and rejected under Discussion on the basis of combined magnetization and Mössbauer evidence. The most probable remaining explanation for the EPR silence of these complexes is extreme heterogeneity in g values ("g strain"), resulting in an EPR signal broadened beyond detection. This remains to be proven through simulation of the "base-line" EPR signal.[3]

Materials and Methods

Buffers and Reagents. The standard buffer was 0.1 M potassium phosphate plus 0.1 mM Na-EDTA at pH 7.7. This buffer was routinely deuteriated (to remove protons) and degassed (to remove oxygen) as described below. Analytical grade reagents were used throughout without further purification.

Enzymes. NADPH-sulfite reductase holoenzyme and its heme protein subunit were isolated from *E. coli* B12 with minor modifications[4] of the procedure of Siegel and Davis (1974). The bacteria were grown on minimal media (Grain Processing Corp., Muscatine, IA) and stored as 2.5-kg cakes at 77 K until used. Following isolation, the heme protein was concentrated to 100 μM in heme and kept at −20 °C in standard buffer. SiR-HP concentrations were determined by using $\epsilon_{591} = 1.8 \times 10^4\ M^{-1}\ cm^{-1}$ (Siegel et al., 1982). The nitrite reductase from *Spinacia oleracea* was prepared by using fresh spinach leaves according to the procedure of Vega and co-workers (Lancaster et al., 1982). This procedure was modified slightly by substituting a phenyl-Sepharose column for the DEAE-Sephadex column. NiR concentrations were determined by using $\epsilon_{386} = 7.6 \times 10^4\ M^{-1}\ cm^{-1}$ (Lancaster et al., 1979).

Removal of Spin $I = {}^1/_2$ Nuclei. Samples were deuteriated to eliminate magnetization noise resulting from the slow relaxation of the spin $I = {}^1/_2$ nuclear paramagnetism of the protons (Day et al., 1987). Deuteriation was accomplished by dilution with standard buffer prepared with 99.8% D_2O followed by concentration using an Amicon unit. Controls were drawn from the filtrate of the final concentration step following deuteriation. Quartz sample holders were used to avoid the spin $I = {}^1/_2$ nuclei common to plastics (e.g., protons in delrin or fluorine in Teflon).

Enzyme Complexes. The sulfite complex of SiR-HP was prepared by reaction of a deuteriated sample of resting enzyme in standard buffer with 40 mM $NaHSO_3$ for 48 h. The nitrite complex of NiR was formed by reaction of a deuteriated sample of resting enzyme in standard buffer with 1 mM $NaNO_2$ for 1.5 h.

Removal of Oxygen. Anaerobic samples were prepared by using standard freeze–pump–thaw techniques employing a rotary pump and highly purified argon (Alphagas UHP argon specified at 99.999% purity).

Magnetization Data. Magnetizations of each sample and its control at fixed fields (5, 2.5, 1.25, and 0.625 T) were collected over the temperature range 1.8–200 K by using a SQUID susceptometer (Quantum Design, San Diego, CA). Matched volumes (0.15 mL) of sample and control in separate, matched (by weight), acid-etched, open quartz holders were used. The Curie region of the difference data at each field was used to find the intercept, which was then set to zero. This removes any mismatch between the sample and its control in their diamagnetism, temperature independent paramagnetism, or ferromagnetic impurities.

The square of the magnetic moment in Bohr magnetons (n_{eff}^2) was calculated from the observed slope of the Curie region (m' in nJ/T per sample), the sample volume (V in milliliters per sample), and the optically determined concentration (c in micromolar) by the equation

$$n_{eff}^2 = 0.537m'/cV$$

Theoretical magnetization curves were calculated as described previously (Day et al., 1987).

The magnetization data, presented in Figures 1, 4, and 5, have not been normalized on a per mole basis. Instead, the results are presented in SI units as nJ/T per sample (ordinate) versus the dimensionless quantity $\beta H/kT$ (abscissa). Theoretical curves have been scaled by using the measured amount of protein (cV in nanomoles per sample). This presentation separates the uncertainty in the magnetization measurement (seen in the scatter of the data) from the uncertainty in the protein concentration measurement used to scale the theoretical curves. For clarity, between 20% and 80% of the data points taken at individual fields have been omitted from these figures. This editing has been done without changing the apparent scatter in the data.

[2] The oxidation states of SiR-HP and NiR and their complexes are identified by the superscripts 0, 1−, and 2−, which refer to the oxidized, 1-electron-, and 2-electron-reduced states, respectively (Christner et al., 1983b).

[3] This is being studied by W. R. Dunham, L. J. Young, L. M. Siegel, J. Peterson, J. J. Bonvoisin, and E. P. Day.

[4] L. J. Young, and L. M. Siegel, manuscript in preparation.

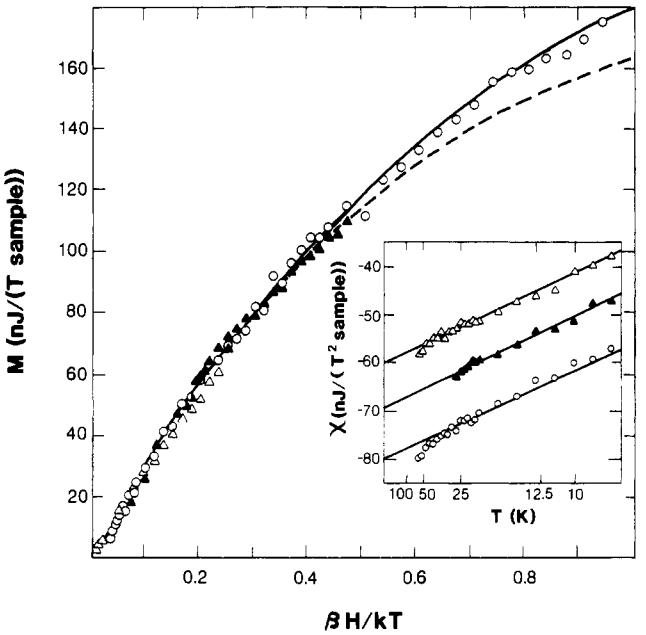

FIGURE 1: Magnetization of the sulfite complex of oxidized *E. coli* sulfite reductase at three fixed fields: (○) 2.5 T; (▲) 1.25 T; (△) 0.625 T. The protein concentration was 0.211 mM. The theoretical curves were found by summing contributions of 97.6% spin $S = {}^1/_2$ and 2.4% spin $S = {}^5/_2$ with the sum scaled to 32 nmol of spin. Both theoretical curves assume $\sum g^2 = 16$ for the spin $S = {}^1/_2$ state. The solid curve assumes (1.7, 2.3, 2.8) for the g values of the spin $S = {}^1/_2$ state, while the dashed curve assumes (0, 0, 4) for these g values. (Inset) High-temperature difference data for the sulfite complex of oxidized sulfite reductase. The results of the least-squares fits to the Curie regions are tabulated below:

	field (T)	points included (from left)	slope (μJ K/T^2 per sample)	intercept (μJ/T^2 per sample)
○	2.500	3–32	0.184 (3)	−0.0802 (3)
▲	1.250	1–25	0.192 (2)	−0.0796 (3)
△	0.625	3–41	0.187 (2)	−0.0800 (3)

All of the magnetization difference data at high temperatures are shown in the insets of Figures 1, 4, and 5. These data are plotted as sample susceptibility in SI units against inverse temperature. For clarity, the data at lower fields have been offset successively by an additional +10 nJ/T^2 per sample each. The solid lines are least-squares fits to the linear region of the data at each field. The results of these fits are tabulated in each figure legend. The points omitted from the fits were affected either by ferromagnetic impurities in the quartz holders (at high temperatures) or by saturation (at low temperatures).

Spectroscopy. EPR spectra were taken with a Bruker ER 200D spectrometer at a modulation frequency of 100 KHz, modulation amplitude of 1 mT, and an operating frequency of 9.47–9.48 GHz. Sample temperature was controlled with an Air Products Heli-Tran refrigeration unit. The base-line signal found by running the appropriate buffer has been subtracted from each EPR spectrum presented in Figures 2 and 6. Optical spectra were recorded on either an Aminco DW-2 UV–vis spectrophotometer or a Perkin-Elmer Lambda 9 UV–vis–Nir spectrometer.

RESULTS

The saturation magnetization of the sulfite complex of oxidized SiR–HP is presented in Figure 1. Magnetization data were collected at each of three fixed fields (2.5, 1.25, and 0.625 T). The fact that the data at three different fixed fields (isofields) lie on top of one another indicates the sample is predominantly spin $S = {}^1/_2$. Magnetization data of metalloprotein samples in higher spin states will show a nested set of isofield curves due to zero-field splitting (Day et al., 1987) as is observed for oxidized SiR-HP (Figure 4). A diamagnetic sample (spin $S = 0$) will of course yield a horizontal line at all fields.

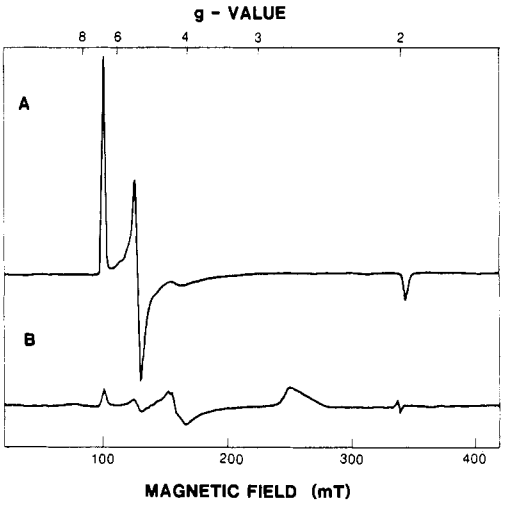

FIGURE 2: (A) EPR spectrum of oxidized *E. coli* sulfite reductase sample before addition of sulfite. The protein concentration was 0.242 mM. Sample temperature was 10 K (nominal). Spectrometer power was 20 mW, and receiver gain was 1.25 × 10^4. (B) EPR spectrum for the sulfite complex of oxidized *E. coli* sulfite reductase whose magnetization is shown in Figure 1. The protein concentration was 0.211 mM. Sample temperature was 10 K (nominal). Spectrometer power was 20 mW, and receiver gain was 5.5 × 10^4.

The data in Figure 1 were collected on a sample containing only 32 nmol of protein (a volume of 0.15 mL at a concentration of 0.211 mM). This is 20 times less than that used previously (0.105 mL at 6.55 mM) in a study of a spin $S = {}^1/_2$ state of a metalloprotein (Petersson et al., 1980). High-quality data on low-concentration metalloprotein samples can now be acquired because a major noise source (spin $I = {}^1/_2$ protons) has been eliminated through deuteriation of the buffer (Day et al., 1987).

The EPR spectrum of oxidized SiR-HP is shown in Figure 2A, and that of the magnetization sample of the sulfite complex of oxidized SiR-HP is shown in Figure 2B. Integration of the spin $S = {}^5/_2$ signal of the oxidized protein in Figure 2B indicates that approximately 2% of the sulfite complex sample was in the uncomplexed state. The small, broad spin $S = {}^1/_2$ signal in Figure 2B that peaks at $g_z = 2.7$ is difficult to quantitate without knowning g_x and g_y (Aasa & Vanngard, 1975). If we assume values typical of low-spin ferrihemes with $\sum g^2 = 16$ (Salerno & Leigh, 1984, and references cited therein), the integrated intensity of this signal is 0.08(2) electrons (De Vries & Albracht, 1979). The EPR spectrum of Figure 2B also contains a very weak signal at $g = 4.3$, indicative of spin $S = {}^5/_2$ impurity.

Most samples of the sulfite complex of oxidized SiR-HP have shown no signal in the vicinity of $g_z = 2.7$ nor any other attributable to a spin $S = {}^1/_2$ state. The weak signal at $g = 2.7$ in Figure 2B is typical of samples prepared recently by using slightly modified isolation procedures.[4]

The Mössbauer spectrum of the sulfite complex of oxidized sulfite reductase at 4.2 K in a parallel field of 60 mT is shown in Figure 3.[5] The quadrupole doublet of the diamagnetic

[5] This Mössbauer spectrum was collected by J. Christner and E. Münck on a sample prepared by P. Janick and L. Siegel. It appears in the Ph.D. thesis of J. Christner (Christner, 1983) and is presented here with her permission.

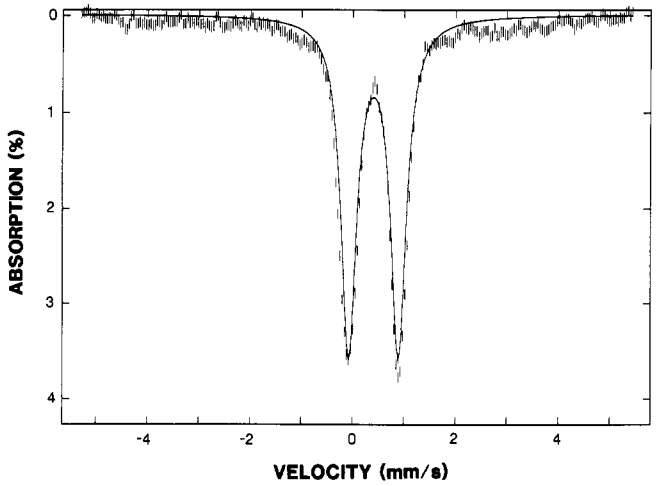

FIGURE 3: Mössbauer spectrum of an ^{57}Fe-enriched sample of the sulfite complex of oxidized *E. coli* sulfite reductase taken at 4.2 K in 60-mT parallel field.[5] The quadrupole doublet indicated by the solid lines was calculated by assuming a quadrupole splitting of 0.97 mm/s, isomeric shift of 0.43 mm/s, and line width of 0.36 mm/s. This doublet has been scaled to 80% of the observed area of the absorption signal.

$[4Fe\text{-}4S]^{2+}$ cluster corresponds to 80% of the absorption area. This is shown by the solid line that was calculated by assuming a quadrupole splitting of 0.97 mm/s, an isomeric shift of 0.43 mm/s, and a line width of 0.36 mm/s. The remaining 20% of the absorption intensity appearing as a pair of broad shoulders between −4.7 and +5.6 mm/s is due to the siroheme iron and is indicative of a paramagnetic, half-odd-integer (Kramers) state.

The square of the magnetic moment of SiR-HP^0-SO_3^{2-} determined from the slope of the Curie region of the magnetization data of Figure 1 (inset) and the optically measured protein concentration is $n_{eff}^2 = 4.74$. The fit to the Curie region of the data in Figure 1 was found by apportioning this observed moment between the spin $S = {}^1/_2$ state ($n_{eff}^2 = 4$) and the spin $S = {}^5/_2$ state ($n_{eff}^2 = 35$). (The choice of $n_{eff}^2 = 4$ for the spin $S = {}^1/_2$ moment is based on the assumption that $\sum g^2 = 16$.) The solid and dashed lines are each sums of 97.6% spin $S = {}^1/_2$ and 2.4% spin $S = {}^5/_2$. The differences between the solid and dashed lines are explained in the legend of Figure 1 and later in the text. The amount of spin $S = {}^5/_2$ found from the fit to the saturation magnetization data (2.4%) is consistent with that indicated by the EPR spectrum of Figure 2B arising from uncomplexed protein (2%) and impurity iron (<1%).

Combined, the magnetization data of Figure 1 and the Mössbauer spectrum of Figure 3 determine that the sample is essentially (97.6%) spin $S = {}^1/_2$. Any alternative interpretation of the magnetization data of Figure 1 would require that a substantial fraction of the siroheme iron be diamagnetic since the observed n_{eff} of 4.74 is less than the moment from any sign higher than spin $S = {}^1/_2$. (For example, for spin $S = 1$, $n_{eff}^2 = 8$.) However, since only 80% of the absorption area of the low-temperature Mössbauer spectrum of Figure 3 is in the form of quadrupole doublets, integer spin for the siroheme iron (including spin $S = 0$) is ruled out.

The interpretation that the sample is predominantly (97.6%) spin $S = {}^1/_2$ is strongly supported by the superposition of the magnetization isofield curves in Figure 1, justified by the close match between the theory (solid line) and the magnetization data of Figure 1, required by the magnetic Mössbauer spectrum of the siroheme iron in Figure 3, and consistent with the optical changes indicating a transition from spin $S = {}^5/_2$ to spin $S = {}^1/_2$ upon formation of the sulfite complex (Janick et al., 1983). Given this overwhelming evidence for the spin $S = {}^1/_2$ state of the sample, it is striking that the EPR spectrum of Figure 2B lacks an appreciable EPR signal attributable to this spin $S = {}^1/_2$ state.

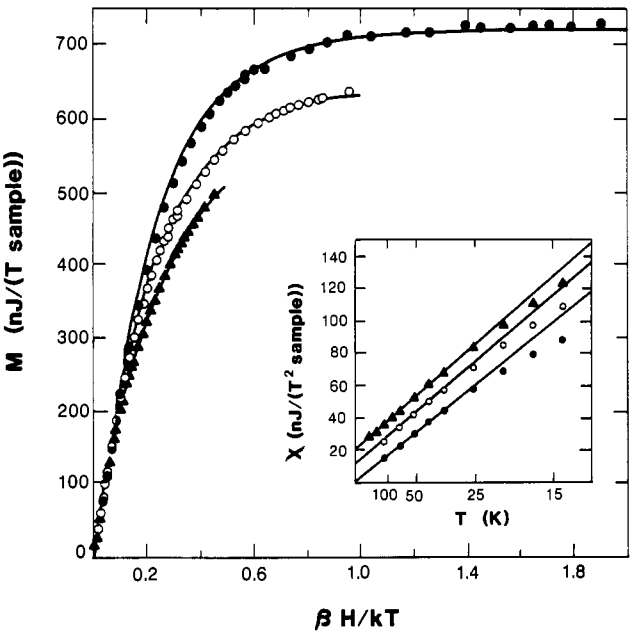

FIGURE 4: Magnetization of oxidized *E. coli* sulfite reductase at three fixed fields: (●) 5 T; (○) 2.5 T; (▲) 1.25 T. The protein concentration was 0.248 mM. The three solid lines through the data are magnetization curves calculated from the spin Hamiltonian given in the text for spin $S = {}^5/_2$ with $D = 8$ cm^{-1} and $E/D = 0.029$. The theoretical curves have been scaled to correspond to 37 nmol of spin. (Inset) High-temperature difference data for oxidized sulfite reductase. The results of the least-squares fits to the Curie regions are tabulated below:

	field (T)	points included (from left)	slope (μJ K/T^2 per sample)	intercept (μJ/T^2 per sample)
●	5.000	1–5	1.48 (1)	+0.0000 (3)
○	2.500	1–5	1.57 (3)	+0.0008 (5)
▲	1.250	1–8	1.61 (1)	−0.0003 (2)

For completeness and as a check on the new magnetization techniques being used here (Day et al., 1987), we have measured the saturation magnetization of oxidized SiR-HP (Figure 4). Previous EPR (Siegel et al., 1973) and Mössbauer studies (Christner et al., 1981) have established that oxidized siroheme is spin $S = {}^5/_2$ with $D = 8 \pm 1$ cm^{-1} and $E/D = 0.029$ and that the [4Fe-4S] cluster is in the diamagnetic ($S = 0$) oxidized state but is exchange coupled to the siroheme. The solid lines of Figure 4 are theoretical curves calculated from the spin $S = {}^5/_2$ Hamiltonian

$$H = D\{[S_z^2 - {}^{35}/_{12}] + (E/D)(S_x^2 - S_y^2)\} + g_0\beta\mathbf{S}\cdot\mathbf{H}$$

with $g_0 = 2$ and the stated zero-field parameters for oxidized SiR-HP. The protein concentration [0.252 (8) mM] found by optimizing the fit of the theory to the data was within the uncertainties of that measured optically [0.248 (5) mM].

It is clear from the quality of the fit of the theory to the data in Figure 4 that saturation magnetization data give results consistent with EPR and Mössbauer spectra and can be used to measure the spin and zero-field splitting of unknown metalloprotein states.

The inset of Figure 4 contains all of the high-temperature, Curie region magnetization data plotted on an expanded scale as susceptibility ($\chi = M/H$) versus inverse temperature. These data are linear up to 200 K (the highest temperature measured), indicating that any excited states populated at this temperature have the same spin as the ground states for both

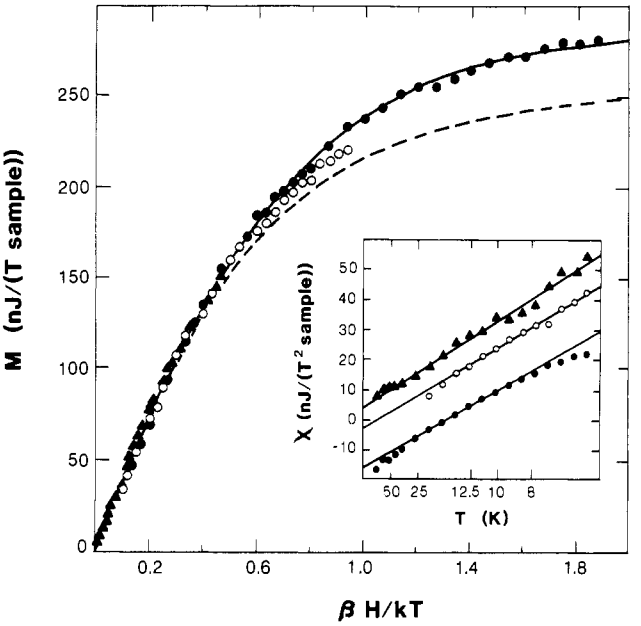

FIGURE 5: Magnetization of the nitrite complex of oxidized spinach nitrite reductase at three fixed fields: (●) 5 T; (○) 2.5 T; (▲) 1.25 T. The protein concentration was 0.293 mM. The theoretical curves are as described in the legend of Figure 1 except there is now 97% spin $S = {}^1/_2$ and 3% spin $S = {}^5/_2$ with the sum scaled to 44 nmol of spin. (Inset) High-temperature difference data for the nitrite complex of oxidized nitrite reductase. The results of the least-squares fits to the Curie regions are tabulated below:

	field (T)	points included (from left)	slope (μJ K/T^2 per sample)	intercept (μJ/T^2 per sample)
●	5.000	6–12	0.256 (3)	−0.0165 (2)
○	2.500	2–16	0.266 (4)	−0.0133 (5)
▲	1.250	4–28	0.286 (4)	−0.0163 (6)

the spin $S = {}^5/_2$ siroheme and the spin $S = 0$ [4Fe-4S] cluster. This sets a lower limit[6] on the exchange coupling within the [4Fe-4S] cluster of $-2J > 290$ cm^{-1}.

The saturation magnetization of the nitrite complex of oxidized NiR is given in Figure 5. A similar procedure to that used in fitting the Curie region of Figure 1 (for the magnetization of the sulfite complex of sulfite reductase) has been used to determine that this sample is 97% spin $S = {}^1/_2$ and 3% spin $= {}^5/_2$.

The EPR spectrum of this sample of the nitrite complex of oxidized NiR is given in Figure 6B. Figure 6A is the EPR spectrum of oxidized NiR before the nitrite is added to form the complex. The EPR spectrum of Figure 6A was run at approximately half the concentration and twice the gain as Figure 6B. Each spectrum contains approximately 13% spin $S = {}^1/_2$ with g values ("1.81", 2.33, 2.70).[7] This low-spin species is often present in the isolated oxidized protein and does not form a nitrite complex. There is no other spin $S = {}^1/_2$ species in the EPR spectrum of the nitrite complex of NiR shown in Figure 6B. Integration of the spin $S = {}^5/_2$ species gives approximately 0.5% for the high-spin oxidized signal and 4% for the impurity iron signal at $g = 4.3$.

[6] The spectrum of states in the spin manifold of a $[4Fe\text{-}4S]^{2+}$ cluster is not known. If we assume that the electrons in the two delocalized pairs are strongly delocalized (Aizman & Case, 1982), then the spin manifold is well-defined with the integer spin states ($S = 0, 1, 2, \ldots, 9$) ordered in increasing energy. The first excited state is then $-2J$ above the ground state. With this assumption, the Curie behavior to 200 K sets a lower limit of 290 cm^{-1} on the antiferromagnetic exchange coupling ($-2J$).

[7] The g_x value in quotation marks was not observed in the EPR spectrum. It was calculated from the observed values and the assumption that $\sum g^2 = 16$.

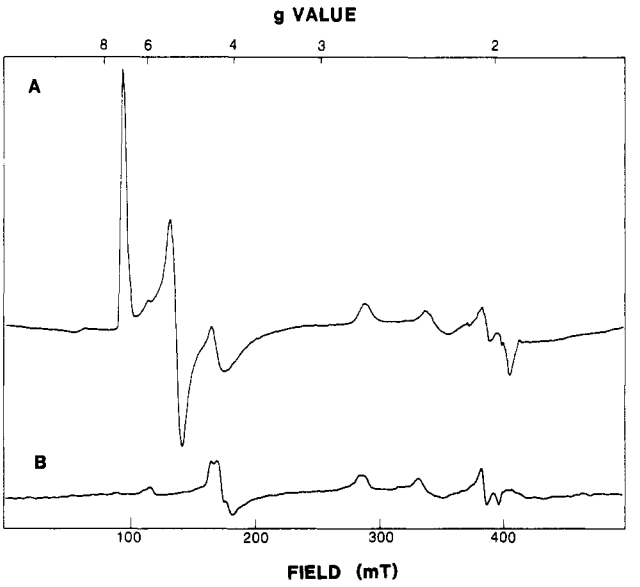

FIGURE 6: (A) EPR spectrum of oxidized spinach nitrite reductase. Protein concentration was 0.0558 mM. Sample temperature was 16 K. Spectrometer power was 2 mW, and receiver gain was 5×10^5. (B) EPR spectrum of the nitrite complex of oxidized spinach nitrite reductase whose magnetization is shown in Figure 5. Protein concentration was 0.118 mM. Sample temperature was 16 K. Spectrometer power was 2 mW, and receiver gain was 2.5×10^5.

The magnetization (3%) and EPR (4.5%) results are consistent in indicating a spin $S = {}^5/_2$ contribution of approximately 3% for this sample of the nitrite complex of oxidized NiR. The EPR spectrum indicates another 13% of the protein is in the low-spin uncomplexed state. The dramatic difference in the two results is that the magnetization data of Figure 5 indicate that the nitrite complex itself (the remaining 84% of the signal) is spin $S = {}^1/_2$, while the EPR spectrum shows no signal for this spin $S = {}^1/_2$ state.

Discussion

When the EPR signal of an expected spin $S = {}^1/_2$ state is not detected, this is usually evidence for a neighboring spin. The neighbor can either broaden the expected spin $S = {}^1/_2$ EPR signal beyond detection by relaxation effects or it can effectively remove the spin $S = {}^1/_2$ state through exchange coupling to form a different system spin. Both of these possibilities can be ruled out as explanations for the EPR silence of the sulfite complex of oxidized SiR-HP.

On the one hand, relaxation broadening by a neighboring spin is excluded (1) by the low-temperature Mössbauer spectrum of the siroheme iron in Figure 3 that is magnetic (indicative of a Kramers system and slow relaxation) and (2) by the magnetization data of Figure 1 that limit the total magnetization of the sample to less than $n_{eff}^2 = 4.74$. Mössbauer transitions occur on a slower time scale (10^{-7} s) than EPR (10^{-10} s) transitions. Thus, when relaxation is slow on the Mössbauer time scale, it is most certainly slow on the EPR time scale. In addition, the magnetization data "has room for" just slightly more than one spin $S = {}^1/_2$ state in the sample. It cannot accommodate the moment of the hypothetical neighbor in addition to that of the spin $S = {}^1/_2$ state of SiR-HP and the 2% of the sample in the spin $S = {}^5/_2$ state of uncomplexed protein.

On the other hand, exchange coupling of the siroheme to the spin $S = 0$ [4Fe-4S] cluster does occur. This exchange interaction leaves the coupled system in a spin $S = {}^1/_2$ state as evidenced by the saturation magnetization data of Figure 1. To determine whether this coupling can result in the EPR silence of the system spin $S = {}^1/_2$ state, we will first examine

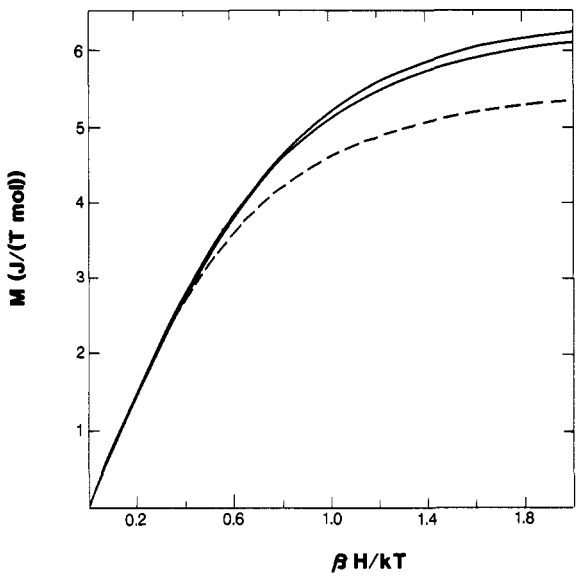

FIGURE 7: Theoretical magnetization curves for low-spin ferrihemes at $H = 5$ T. In each case, $\sum g^2 = 16$. The lowest (dashed) curve has $g = (0, 0, 4)$. The middle (solid) curve has $g = (0.93, 1.89, 3.45)$. The top (solid) curve has $g = (1.72, 2.22, 2.80)$.

the effects of the coupling in oxidized SiR-HP.

The coupling model used to explain oxidized SiR-HP has been discussed at length (Christner et al., 1981; Münck, 1982; Christner, 1983). For the present purposes, the crucial observation is that the magnetic properties (measured by EPR, Mössbauer, and saturation magnetization data) of the system spin $S = {}^5/_2$ state of oxidized SiR-HP are typical of high-spin ferric hemes. In this case the coupling has not measurably affected the magnetic properties of the siroheme. The coupling does affect the properties of the cluster dramatically by mixing its spin $S = 1$ excited states with its spin $S = 0$ ground state. The result is a polarization of the spins of the cluster iron sites proportional to the spin of the siroheme. This results in magnetic Mössbauer spectra for the cluster at low temperatures despite the fact its spin is $S = 0$. The reason for this intrinsic asymmetry (the cluster is affected but the siroheme is not) in the impact of the cluster–siroheme coupling is the low-lying excited states of the cluster (100–400 cm^{-1}) compared with the relatively large gap (2000–10000 cm^{-1}) between the ground state and the first excited state of the siroheme.

Now consider the sulfite complex of oxidized SiR-HP and a hypothetical, uncoupled, but otherwise similar complex. For the observed system spin $S = {}^1/_2$ state to differ from that of the analogous complex of uncoupled siroheme, there must be a low-lying excited state of the siroheme sulfite complex. The coupling to the cluster would mix this excited state with the ground state, changing the EPR properties of the system state from that of the uncoupled siroheme complex.

There is evidence that this does not occur. For example, the expected spin $S = {}^1/_2$ EPR signals occur at full intensity for the cyanide complexes of the oxidized and doubly reduced states of SiR-HP and for the carbon monoxide complex of the doubly reduced state (Siegel et al., 1982; Janick & Siegel, 1983). In these cases, one or the other of the siroheme or [4Fe-4S] cluster is diamagnetic (spin $S = 0$) and coupled to its partner in a spin $S = {}^1/_2$ state to produce a spin $S = {}^1/_2$ system state (Christner et al., 1983b). It is only the physiological substrate complexes with the oxidized metalloproteins that are EPR silent (Vega & Kamin, 1977; Janick et al., 1983; Young & Siegel, 1988) when the system spin is $S = {}^1/_2$.

There are at least two other possible explanations for the EPR silence of the spin $S = {}^1/_2$ state of the SiR-HP complexes: either (1) the spin state has a well-defined set (g_x, g_y, g_z) of g values that is so anisotropic it cannot be detected using EPR, as would be the case, for example, with $g = (0, 0, 4)$ (in this case there is no g strain, but there is extreme anisotropy) or (2) the sample is heterogeneous having a wide range of g values (g strain), resulting in an EPR signal broadened beyond detection under standard conditions. The shape of the saturation magnetization curve differs significantly in these two situations as shown in Figure 7, where three 5-T magnetization curves for spin $S = {}^1/_2$ states having different sets of g values are depicted. In each case $\sum g^2 = 16$. The dashed curve has $g = (0, 0, 4)$. The upper two solid curves have quite distinct g_z values of $g_z = 3.45$ (middle curve) and $g_z = 2.80$ (upper curve) despite the fact the curves themselves are very similar. The magnetization curves for all spin $S = {}^1/_2$ states with $\sum g^2 = 16$ and $g_z < 3.5$ lie in the vicinity of the two, nearly identical, upper curves.

The magnetization data of Figure 1 rule out extreme anisotropy as an explanation for the EPR silence of the spin $S = {}^1/_2$ state of the sulfite complex of oxidized SiR-HP since the dashed curve with $g = (0, 0, 4)$ does not match the data. On the other hand, a spread in g_z values from 3.5 to 2.8 is compatible with the magnetization data (solid line). This explanation for the lack of EPR signal is at least consistent with the observed, but small, EPR signal intensity in the vicinity of $g_z = 2.7$.

By analogy with the SiR-HP^0-SO_3^{2-} complex, the absence of a spin $S = {}^1/_2$ signature in the EPR spectrum of Nir^0-NO_2^- is not a consequence of relaxation broadening or exchange coupling to the [4Fe-4S] cluster.

Several explanations have been advanced to account for the low intensity (or absence) of EPR signals attributable to nitrite complexes of ferric heme proteins. Most of these explanations can be ruled out in the present case by the magnetization data. For example, the formation of the diamagnetic ferric nitrosyl complex (through either autoreduction or some other protein-mediated process) is ruled out by the fact the spin $S = {}^1/_2$ state is observed and accounts for more than 95% of the total protein. As for SiR-HP^0-SO_3^{2-}, an extremely anisotropic spin $S = {}^1/_2$ system [$g = (0, 0, 4)$] can also be excluded for Nir^0-NO_2^- since this does not fit the data (dashed lines of Figure 5). This again leaves extreme heterogeneity (g strain) as the remaining explanation for the "missing" EPR intensity.

Whether such a spread in g values leads to an EPR signal broadened beyond detection (at least under standard recording conditions) remains to be shown. A thorough study of the EPR spectrum of the SiR-HP^0-SO_3^{2-} complex at various microwave frequencies and employing different instrument recording modes, together with spectral simulations, is under way.[3] The significance of the present observations will remain whatever the outcome of the EPR study. Namely, the absence of EPR signal intensity can no longer be taken as evidence for the absence of a spin $S = {}^1/_2$ state—especially in the case of the sulfite or nitrite siroheme adducts.

ACKNOWLEDGMENTS

We thank Jodie Christner and Eckard Münck for use of the low-temperature Mössbauer spectrum of the sulfite complex of oxidized sulfite reductase in Figure 3.

REFERENCES

Aasa, R., & Vanngard, T. (1975) *J. Magn. Reson. 19*, 308–315.

Aizman, A., & Case, D. A. (1982) *J. Am. Chem. Soc. 104*, 3269–3279.

Christner, J. A. (1983) Ph.D. Thesis, University of Minnesota.

Christner, J. A., Münck, E., Janick, P. A., & Siegel, L. M. (1981) *J. Biol. Chem. 256*, 2098-2101.
Christner, J. A., Münck, E., Janick, P. A., & Siegel, L. M. (1983a) *J. Biol. Chem. 258*, 11147-11156.
Christner, J. A., Janick, P. A., Siegel, L. M., & Münck, E. (1983b) *J. Biol. Chem. 258*, 11157-11164.
Christner, J. A., Münck, E., Kent, T. A., Janick, P. A., Salerno, J. C., & Siegel, L. M. (1984) *J. Am. Chem. Soc. 106*, 6786-6794.
Cline, J. F., Janick, P. A., Siegel, L. M., & Hoffman, B. M. (1985) *Biochemistry 24*, 7942-7947.
Day, E. P., Kent, T. A., Lindahl, P. A., Münck, E., Orme-Johnson, W. H., Roder, H., & Roy, A. (1987) *Biophys. J. 52*, 837-853.
De Vries, S., & Albracht, S. P. J. (1979) *Biochim. Biophys. Acta 546*, 334-340.
Janick, P. A., & Siegel, L. M. (1983) *Biochemistry 22*, 504-515.
Janick, P. A., Rueger, D. C., Krueger, R. J., Barber, M. J., & Siegel, L. M. (1983) *Biochemistry 22*, 396-408.
Lancaster, J. R., Vega, J. M., Kamin, H., Orme-Johnson, N. R., Orme-Johnson, W. H., Krueger, R. J., & Siegel, L. M. (1979) *J. Biol. Chem. 254*, 1268-1272.
Lancaster, J. R., Batie, C. J., Kamin, H., & Knaff, D. B. (1982) in *Methods in Chloroplast Molecular Biology* (Edelman, J., Halleck, K. B., & Chua, N.-H., Eds.) pp 723-734, Elsevier Biomedical, Amsterdam.
McRee, D. E., Richardson, D. C., Richardson, J. S., & Siegel, L. M. (1986) *J. Biol. Chem. 261*, 10277-10281.
Münck, E. (1982) in *Iron-Sulfur Proteins* (Spiro, T. G., Ed.) pp 147-175, Wiley, New York.
Murphy, M. J., Siegel, L. M., Tove, S. R., & Kamin, H. (1974) *Proc. Natl. Acad. Sci. U.S.A. 71*, 612-616.
Petersson, L., Cammack, R., & Rao, K. K. (1980) *Biochim. Biophys. Acta 622*, 18-24.
Salerno, J. C., & Leigh, J. S. (1984) *J. Am. Chem. Soc. 106*, 2156-2159.
Siegel, L. M. (1978) in *Mechanisms of Oxidizing Enzymes* (Singer, T. P., & Ondarza, R. N., Eds.) pp 201-214, Elsevier, New York.
Siegel, L. M., & Davis, P. S. (1974) *J. Biol. Chem. 249*, 1587-1598.
Siegel, L. M., Murphy, M. J., & Kamin, H. (1973) *J. Biol. Chem. 248*, 251-264.
Siegel, L. M., Rueger, D. C., Barber, M. J., Krueger, R. J., Orme-Johnson, N. R., & Orme-Johnson, W. H. (1982) *J. Biol. Chem. 257*, 6343-6350.
Vega, J. M., & Kamin, H. (1977) *J. Biol. Chem. 252*, 896-909.
Wilkerson, J. O., Janick, P. A., & Siegel, L. M. (1983) *Biochemistry 22*, 5048-5054.
Young, L. J., & Siegel, L. M. (1988) *Biochemistry* (in press).

Effect of Unfolding on the Tryptophanyl Fluorescence Lifetime Distribution in Apomyoglobin

E. Bismuto,[‡] E. Gratton,[§] and G. Irace*[,‡]

Cattedra di Chimica e Propedeutica Biochimica, Istituto di Chimica e Chimica Biologica, I Facoltà di Medicina e Chirurgia, Università di Napoli, Via Costantinopoli 16, 80138 Napoli, Italy, and Department of Physics, University of Illinois at Urbana-Champaign, 1110 West Green Street, Urbana, Illinois 61801

Received August 5, 1987; Revised Manuscript Received October 16, 1987

ABSTRACT: Proteins exhibit, even in their native state, a large number of conformations differing in small details (substates). The fluorescence lifetime of tryptophanyl residues can reflect the microenvironmental characteristics of these subconformations. We have analyzed the lifetime distribution of the unique indole residue of tuna apomyoglobin (Trp A-12) during the unfolding induced by temperature or guanidine hydrochloride. The results show that the increase of the temperature from 10 to 30 °C causes a sharpening of the lifetime distribution. This is mainly due to the higher rate of interconversion among the conformational substates in the native state. A further temperature increase produces partially or fully unfolded states, resulting in a broadening of the tryptophanyl lifetime distribution. The data relative to the guanidine-induced unfolding show a sigmoidal increase of the distribution width, which is due to the transition of the protein structure from the native to the random-coiled state. The broadening of the lifetime distribution indicates that, even in the fully unfolded protein, the lifetime of the tryptophanyl residues is influenced by the protein matrix, which generates very heterogeneous microenvironments.

Guanidine hydrochloride is a powerful denaturing agent for proteins. Native globular proteins usually undergo a marked structural transition in the presence of guanidine. Generally, the transition is completed at a denaturant concentration ranging between 6 and 8 M at room temperature, except for some exceptionally stable proteins (Pace, 1975). When the transition is completed, proteins are found to be random coiled, without any residual ordered structure (Tanford, 1968). In these conditions, the spectroscopic properties of the aromatic residues are supposed to be similar to those of the monomeric amino acids in water (Demchenko, 1986).

A protein molecule, in a particular conformational state, can assume a very large number of substates, rapidly interconverting at room temperature, having the same coarse overall structure but differing in small structural details. For example,

[‡] Università di Napoli.
[§] University of Illinois at Urbana-Champaign.

0006-2960/88/0427-2132$01.50/0